Distinguishing Between the Pitting Corrosion Behaviour of 316L(N) and 316 Stainless Steels Using Shot Noise Analysis

M.G. Pujar, N. Parvathavarthini, Sidhartha S. Jena*, B.V.R. Tata* and R. K. Dayal
Corrosion Science and Technology Division (CSTD)
*Materials Science Division (MSD)
Indira Gandhi Centre for Atomic Research (IGCAR)
Kalpakkam – 603 102.

Abstract

In the present work, an attempt has been made to analyze Electrochemical Noise (EN) data obtained from 316 Stainless Steel (SS) and 316L(N) coupons exposed to aerated 0.5M NaCl solution for 30d. The analysis of the data was based on the principle of stochastic process like pitting corrosion. Initially, the cumulative probability of the frequency of pitting corrosion events was numerically calculated which was transformed from the domain of the frequency of events to the mean free time domain. Thereupon, Weibull probability plot was constructed by fitting Weibull distribution function to the calculated cumulative probability. From the slopes and the intercepts of the Weibull plots, the pit embryo generation rate was calculated. The data analysis was conducted after the exposure of 10, 15 and 20d respectively so as to examine the distinguishing features that could be obtained from the Weibull probability plots. It was observed that, 316SS showed ever growing pitting corrosion events which was reflected in the Weibull probability plots. However, 316L(N) showed passivation after a few events of metastable pitting (10d exposure) which was reflected in the Weibull probability plots. The pit embryo generation rate was found to be suppressed in 316L(N) which signified the true reason for its showing enhanced pitting corrosion resistance.

Keywords: Electrochemical noise, Stainless steel, Shot noise, Pitting corrosion

Introduction

Type 316L(N) Austenitic Stainless Steel is the currently favoured structural material in the primary side of Prototype Fast Breeder Reactor (PFBR). The choice of this material is based on its resistance to sensitization and adequate high temperature mechanical properties. It is being used in many structural components such as main vessel, safety vessel, inner vessel, auxiliary grid plate, fuel transfer machines, intermediate heat exchangers and core support structures because of its adequate strength, corrosion resistance, good weldability and compatibility with liquid sodium. Low carbon grades have been chosen to ensure freedom from sensitization during welding of the components and to avoid the risk of chloride stress corrosion cracking during storage in coastal site of Kalpakkam. Since low carbon grades have lower strength than normal grades, nitrogen is specified as an alloying element to improve the mechanical properties so that the strength is comparable to 316 SS.

However, it is reported that several austenitic steels suffer extensive pitting or localized corrosion in the presence of halide ions [1]. Various alloying elements have been added to stainless steel, but only Cr, Mo and N were found to be effective in promoting the resistance to localized corrosion [2]. The beneficial effects of nitrogen, as an alloying element, towards the mechanical and corrosion properties of many austenitic SS have been well recognized over the last two decades. In particular, it has been reported that nitrogen alloying can lead to improvements in pitting resistance of the alloys in Cl^- ion-bearing neutral and acidic solutions [3, 4]. It is also well known that the accelerated DC corrosion tests like potentiodynamic anodic polarization studies conventionally used to determine the pitting potential (E_{pp}) of an alloy in a given medium can lead to the irreversible changes or damage to the specimen due to the dissolution during active polarization and hence are not preferred sometimes. It is reported that the same passive film on a specimen rarely showed a definite E_{pp} value as E_{pp} has a statistical character [5]. Thus, it becomes obvious that the E_{pp} values of the alloys determined using DC technique are not the true indicators of the pitting corrosion resistance of the alloys under study. Electrochemical noise (EN) technique has become quite popular in recent years most likely due to its perceived advantages over other electrochemical techniques [6-10]. In the recent times, adequate literature is available on EN studies where shot noise analysis technique is employed to distinguish between different forms of corrosion by examining the properties of several of the parameters which were proposed as indicative of the type of corrosion [11-13].

In the present paper, attempt has been made to study the effect of long-term exposure of 316SS and 316L(N) to aerated 0.5M NaCl solution using EN technique. Shot noise analysis technique was employed to analyze the current and potential noise data to obtain Weibull probability plots; thereby it was possible to distinguish between the localized corrosion resistance of 316SS and 316L(N) based on the distinct pit embryo generation rates of the steels.

Experimental

The chemical compositions of the 316SS and 316L(N) SS used in the present work are given in Table 1. In order to avoid crevice corrosion attack generally observed in the mounted specimens, corrosion coupons (25 mm length, 18 mm breadth and 6mm thickness, drilled and tapped at one end) were used in the present work.

Electrochemical noise studies on these materials were performed using two nominally identical coupons of the same size. The coupons were connected to the EN measurement system (Solartron SI 1287) using threaded specimen rods, which were covered with Teflon tape. The specimens were polished up to 1000 grit finish, washed in soap water and degreased in acetone.

Potential and current noise measurements were performed by shorting together two identical working electrodes. The current flowing between the two working electrodes, as well as the potential between the working electrode and a reference electrode were monitored. The area of the specimen exposed to the solution was about 7 cm^2.

The potentiostat, which can perform this experiment actively, holds the working electrode connection at the 'ground' potential by a small amplifier circuit. If one 'working' electrode is directly connected to ground and the other is connected to the working electrode cable, they are both held at the same potential and are, in effect, 'shorted' together. Any current, which flows between the two electrodes, is measured by the instruments of current measurement circuits thus creating a Zero Resistance Ammeter (ZRA). The potential is measured between the 'working' electrodes (since they are shorted together, both 'working' electrodes are at the same potential) and a reference electrode. Saturated calomel electrode (SCE) was used as a reference electrode for the measurement of potential noise.

Electrochemical current and potential noise studies were conducted in aerated 0.5M sodium chloride solution at open circuit potential (OCP) and noise signals were collected at the sampling frequency of 1 Hz. The experiment was performed over a period of 30 days in order to get the information on the pitting corrosion behaviour of the specimens during long-term exposure. Since in EN studies, the signal is mostly non-stationary, the drift or the trend gets introduced. Therefore, the drift or the trend removal was carried out using linear detrending technique, which is an accepted practice, before calculating the statistical parameters as well as power spectral density (PSD) values. Three sets of current and potential noise data consisting of 1024 data points were obtained successively daily (at the fixed hour) and analyzed to calculate statistical parameters as well as PSD plots. All the potential and current noise data collected in the time domain were transformed in the frequency domain through the fast Fourier transform (FFT) method, by a dedicated software after suitably detrending. FFT based measurements are subject to errors from an effect known as leakage. This effect occurs when the FFT is computed from of a block of data which is not periodic. To correct this problem appropriate windowing functions must be applied. When windowing is not applied correctly, then errors may be introduced in the FFT amplitude, frequency or overall shape of the spectrum. Since most signals are not periodic in the predefined data block time periods, a window must be applied to correct for leakage. A window is shaped so that it is exactly zero at the beginning and end of the data block and has some special shape in between. This function is then multiplied with the time data block forcing the signal to be periodic. A Windowing function minimizes the effect of leakage to better represent the frequency spectrum of the data. Thus, in order to reduce the

leakage of the low as well as the high frequencies in the calculated PSD values, Hanning window was used for signal analysis.

Confocal Microscopy: After the 30d exposure, the specimens were washed, dried and observed under Leica TCS-SP2-RS (Germany) confocal laser scanning microscope (CLSM), equipped with a Leica DMIRE2 inverted microscope and lasers. The images were taken in reflection mode using Ar^+ ion laser operating at 488 nm and a 40x / 0.75 numerical aperture objective lens. All the images were taken by scanning a frame of 512 x 512 pixels in x-y plane with the laser beam and each image was averaged over 10 frames for better signal to noise ratio. The 3D images were constructed by stacking the 2D images acquired over several micrometers in z-axis.

Data analysis using stochastic theory and shot noise

Usually a large scatter is observed in the measurable parameters like corrosion rate, maximum pit depth, time to perforation etc. during localized corrosion. This scatter results from the influence of metal surface heterogeneities and from variations in the corrosive environment over time during pit growth. All these facts suggest that randomness is an inherent and unavoidable characteristic of pitting corrosion over time, so that stochastic models are better suited to describe pitting corrosion processes. The output obtained using the stochastic models is random or probabilistic. It may be possible to predict the generation probability of events in the future from the past events, which is termed as, “conditional probability” [14].

Shot noise theory is based on the assumption that the current signal is composed of discrete charge carriers [13]. Shot noise is produced when the current takes the form of a series of statistically independent packets of charge, with each packet having a short duration [6]. The number of charge carriers passing a given point will be a random variable. According to the stochastic process the individual events are independent of other events, thus, shot noise analysis is applicable to the individual events [6, 12]. This theory can be applied to the analysis of electrochemical noise data from corrosion processes. If this theory is applied to EN, three parameters can be obtained: I_{corr} the average corrosion current, q the average charge in each event, and f_n frequency of the appearance of these events. Only two of these parameters are independent, since

$$I_{corr} = q * f_n \qquad (1)$$

It is not possible to measure I_{corr} , q and f_n directly, but it is possible to estimate them from the measured current and potential noise [12]. Assuming that shot noise is produced during breakdown of the passive film as well as pit initiation and hydrogen evolution, the q and f_n are given as [14]:

$$q = \frac{\sqrt{PSD_E * PSD_I}}{B} \quad \text{and} \quad q = \frac{\sigma_I \sigma_E}{Bb} \tag{2}$$

$$f_n = \frac{B^2}{PSD_E * A} \quad \text{and} \quad f_n = \frac{B^2 b}{\sigma_E^2} \tag{3}$$

where PSD_E and PSD_I are the low frequency PSD values of the potential and current noise respectively, B is the Stern-Geary coefficient, σ_I and σ_E are the standard deviation values of current and potential respectively and b is the bandwidth of measurement as, standard deviation is a function of measurement bandwidth and A is the surface area of the specimen. The charge q is independent of area and f_n is proportional to area, so it can be reported as events per second per unit area [12]. In these calculations the B value was taken to be 0.026 V per decade [6]. This result is obtained for common values of the Tafel slopes for the anodic and cathodic reactions.

The cumulative probability F(f_n) at each f_n is determined from the set of f_n values calculated using equation 3 given above according to the mean rank approximation [13]. According to this method (using f_n as an example): 1) all the values of f_n were sorted in an ascending order and 2) then the cumulative probability for each value was calculated as n/(N+1), where n is the position in the sorted list, and N is the total number of entries in the list [12]. Similarly, the characteristic charge, q values were calculated as per the equation 2 and cumulative probability F(q) was calculated at each q value.

Pit initiation time will follow a Weibull distribution [15] when it is regarded as the survival time defined as the time to first failure (passive film breakdown) of an individual part or process. Weibull distribution function is one of the frequently used cumulative probability functions for predicting life time in reliability test [14]. Using this distribution it is possible to analyze data even when two or more failure modes are present at the same time [5]. The Weibull distribution is often used in the field of life data analysis due to its flexibility—it can mimic the behavior of other statistical distributions such as the normal and the exponential. The cumulative probability F(t) of a failure system can be written just as Weibull distribution function, which is expressed as [14],

$$F(t) = 1 - \exp(-t^m / n) \tag{4}$$

m and n are the shape and scale parameters, respectively; m is a dimensionless parameter and n is expressed as s^m. Shape parameters allow a distribution to take on a variety of shapes, depending on the value of the shape parameter. The Weibull distribution has a relatively simple distributional form. However, the shape parameter allows the Weibull to assume a wide variety of shapes. The effect of the scale parameter is to stretch out the graph. The equation 4 can be rewritten as follows:

$$\ln\{\ln[1/(1-F(t))]\} = m\ln t - \ln n \qquad (5)$$

By using the cumulative probability values for the localized corrosion events, f_n calculated previously, in the above equation and fitting, two parameters m and n can be determined from the slope of the linear plot of ln{ln[1/(1-F(t))]} versus ln t, (also known as Weibull probability plot) and from the intercept on the ln{ln[1/(1-F(t))]} axis, respectively.

The pit nuclei or embryo generation rate is defined as,

$$r(t) = \frac{m}{n} t^{m-1} \qquad (6)$$

based upon Weibull distribution function. In order to study the progress of pitting or passivation in two stainless steels, the analysis of the data was done after the exposure periods of 10, 15 and 20 days and Weibull probability plots were prepared using the PSD values. The Weibull plot was also prepared by using the standard deviation values for the exposure time of 10d for comparison.

Results and discussion

The cumulative probability of frequency of events, F(f_n) was plotted for 316SS and 316L(N) in aerated 0.5M NaCl solution after the exposure of 10, 15 and 20 days respectively (Fig.1). It has been reported that the parameters q and f_n derived from shot noise theory provide vital information about the nature of the corrosion processes [6, 16]. Thus, q gives an indication of the mass of the metal lost in the event while f_n provides information about the rate at which these events are happening [11]. Localized corrosion, such as pitting, can be characterized by a small number of events, and is therefore expected to have a low frequency and high charge [12]. In the case of passivity, the charge is expected to be low, while the frequency will depend on the processes occurring on the passive film [11].

It has been reported that when the cumulative probability plots do not overlap then it shows that there is good discrimination ability and effectiveness in the parameter studied [13]. It was reported that the cumulative probability plot in the lower cumulative probability range corresponded to dominant pitting corrosion [17].Since the pitting corrosion events have the lower cumulative probability, it would be useful in distinguishing the change in the pitting corrosion resistance of the two alloys from Fig.1; thus, lower the events, higher the pitting corrosion and inferior would be the pitting corrosion resistance of the said alloy in the chloride containing environment. It was observed that the pitting corrosion events were lower for 316SS after 10d exposure. It has been reported that high frequency events generally tend to occur all over the specimen surface, whereas corrosion process would be rather localized when low frequency events are dominant [14]. It was further noted that, as the time of exposure increased, the frequency of pitting corrosion events of 316SS remained

the same, but the corrosion events of 316LN increased by several orders of magnitude at the lower cumulative probability values. It is reported that passive or inhibited specimens have a high value of f_n [12]. It has been reported by Cottis [6] that passive systems showed high or low value of f_n. Thus, it can be inferred that 316L(N) attained the passive state with increase in the exposure time unlike 316SS which underwent severe pitting.

The cumulative probability plots of charge, q values versus the charge values are given in Fig.2. From the viewpoint of the shot noise analysis, the higher the value of q, the more charge in each event, that is, the more mass is being lost in each anodic event. This is also obvious from the fact that the current transients during localized corrosion are large. The q values for 316SS range from 10^{-10} to 10^{-4} C whereas for 316L(N) they range from 10^{-10} to 10^{-5} C after 10 d exposure. However, after 15d and 20 d exposure, the charge values for 316L(N) were calculated to be in the range of 10^{-10} to 10^{-7} and 10^{-10} to 10^{-8} C respectively. On the contrary, the charge values for 316SS remained almost the same during these exposure periods. The high charge values shown by 316SS throughout indicate the progress of pitting corrosion as against the passivation of 316L(N) from the decreasing charge values [6].

Since the stochastic analysis can be applicable only in the time domain, the plots of the cumulative probability of f_n in Fig.1 were transformed from the f_n domain to the $1/f_n$ mean-free time domain before applying the Weibull distribution function to $F(1/f_n)$, in order to study the low frequency events associated with localized corrosion in more detail [17]. The resulting plots of $F(1/f_n)$ versus time were rearranged according to equation 4, which gave the Weibull probability plots (Fig.3). It was observed that Weibull probability plots for the data obtained after exposing 316SS and 316L(N) to aerated 0.5M NaCl solution for 10d showed two distinctly linear regions. Since, it is clear that in aerated 0.5M NaCl solution corrosion can proceed through the modes of localized corrosion and/or passivation, it is suggested that the slopes in the relatively shorter time range are associated with passivation. The slopes in the relatively longer time range are responsible for localized corrosion events such as metastable pitting or stable pitting corrosion [14]. As the time of exposure increased to 15 and 20d, although, the Weibull probability plots for 316SS retained two linear regions, the Weibull probability plots for 316L(N) transformed from two-linear region into a single line, the slopes of which fall into relatively shorter time range. This showed that 316L(N) had gradually passivated as the time of exposure increased, while 316SS continued to undergo stable pitting. The Weibull probability plots obtained using standard deviation is shown in Fig.4; the plots of 316SS and 316L(N) showed two linear regions with some scatter.

The m and n parameters obtained after 10 d exposure by using Weibull plots prepared using PSD values as well as by using the standard deviation values are given in Table 2. Using the values

of m and n obtained from Weibull plots, the pit embryo or nucleation generation rates were calculated using equation 5 and plotted (Fig.5). It was observed that pit embryo generation rates were always higher for 316SS compared to 316L(N); in fact pit embryo generation rate in 316L(N) calculated using Weibull plots prepared from the standard deviations was negligible indicating the suppression of pitting corrosion. Since the values of m shown in Table 2 are less than unity, they result in exponential decay curves for r (t) as a function of time.

Most of the pits in 316SS that were observed under CLSM were found to be circular (but not exclusively, as some of the pits with irregular shapes too were observed) at the opening and were found to have attacked the alloy in a vertical fashion. Pits with as large as 70-80 μm diameters and as deep as 20-25 μm too were observed. The pitting corrosion attack of this nature in the stationary aerated 0.5M sodium chloride solution could be considered to be quite serious in nature. The Fig.6 (a, b) show the 2D and the 3D photomicrographs of a large pit grown on 316SS after the 30 days exposure. The 2D photomicrograph showed a somewhat shiny object at one end of the pit, which could be possibly, an inclusion. The 3D photomicrograph showed that the pit could have got initiated near the inclusion and grown all around it; this picture gives the fair idea about the depth of the pit, which is about 10 μm. Figure 7 (a, b) showed the 2D and the 3D photomicrographs of a shallow pit in 316L(N) after 30 days of exposure. The 2D photomicrograph showed the bright shiny metal, which was nothing but the passivated steel at the shallow pit bottom. The 3D photomicrograph showed the shallowness of the pitting attack along with the polishing lines that were visible even through the pit interior, indicating a shallow pit, which got repassivated and stopped growing. The depth measurement of some of the pits observed in 316L(N) steel could not be accomplished satisfactorily owing to the fact that, the depths of these pits were less than 300 nm; thus, it showed that the pits which got initiated did not grow further and got repassivated. This behaviour reflected in the Weibull probability plots obtained after 15 and 20d. Thus, it was possible to clearly distinguish between the pitting corrosion resistance of 316SS and 316L(N) exposed to aerated 0.5M NaCl solution using the concepts of shot noise theory and Weibull probability plots; the results obtained from these calculations concurred well with the CLSM photomicrographs of the exposed specimens.

Conclusions

From the EN studies conducted on 316SS and 316L(N) exposed to aerated 0.5M NaCl solution for 30d following conclusions were drawn:

1. The shot noise analysis of EN data obtained after 10, 15, 20d revealed that cumulative probability plots of f_n and q was very helpful in making a good discrimination between the corrosion resistance of the above steels. The cumulative probability plots of f_n showed that 316SS

continued to undergo pitting corrosion, however, 316L(N) passivated after showing signs of undergoing metastable pitting initially.

2. The Weibull probability plots for the above steels showed two distinctly linear regions; the region at the shorter time duration indicated passivation in the chloride containing environment whereas the region at the longer time duration indicated localized corrosion like pitting.
3. Pit embryo generation rates were calculated using the parameters m and n which were obtained from the Weibull probability plots; these plots showed that the pit embryo generation is suppressed in 316L(N) compared to 316SS. This was supported by the CLSM photomicrographs.
4. Thus, more comprehensive information about the localized corrosion aspects of both steels could be obtained by conducting shot noise analysis. These data were found to be far more informative than the E_{pp} values generally obtained in the laboratories.

References

1. M. G. Fontana (Ed.), Corrosion Engineering, McGraw-Hill, New York, USA, 1987, p 71.
2. L. L. Shreir, R. A. Jarman, G.T. Burstein (Eds.), Corrosion, Vol. 1, Metal/Environment Reactions, 3rd ed., Butterworth-Heinemann, Oxford (1994) p 3:47.
3. G.C. Palit , V. Kain, and H.S. Gadiyar, Corrosion 49 (1993) 977.
4. R. F. A. Jargelius-Pettersson, Corros. Sci. 41 (1999) 1639.
5. S.-I Pyun and E.-J Lee, Surface and Coating Technology 62 (1993) 480.
6. R.A. Cottis, Corrosion 57 (2001) 265.
7 D. A. Eden, CORROSION/98, paper no.386, National Association of Corrosion Engineers, Houston, Texas, 1998
8. J. Smulko and K. Darowicki, Journal of Electroanalytical Chemistry 545 (2003) 59.
9. Aballe, M. Bethencourt, F.J. Bonata, and M. Marcos, Electrochim. Acta 44 (1999) 4805.
10. U. Bertocci, C. Gabrielli , F. Huet, and M. Keddam, J. Electrochem. Soc. 144 (1997) 31.
11. R.A. Cottis, M.A. A. Al-Awadhi, H. Al-Mazeedi and S. Turgoose, Electrochimica Acta 46 (2001) 3665.
12. H. A. A. Al-Mazeedi and R. A. Cottis, Electrochimica Acta 49 (2004) 2787.
13. J. M. Sanchez-Amaya, R. A. Cottis and F. J. Botana, Corros. Sci. 47 (2005) 3280.
14. K.-H Na, S.-II Pyun and H.-P Kim, Corros. Sci. 49 (2007) 220.
15. A. Valor, F. Caleyo, L. Alfonso, D. Rivas and J. M. Hallen, Corros. Sci. 49 (2007) 559.
16. R. A. Cottis and S. Turgoose, Materials Science Forum 192-194 (1995) 663.
17. K.-H. Na and S.-I Pyun, Corrosion Science 50 (2008) 248.

Table 1: Chemical composition of the stainless steels, wt. %.

Element	316SS	316L(N)
C	0.050	0.025
Cr	16.92	18.16
Ni	11.67	11.9
Mo	2.19	2.4
N	------	0.067
Mn	1.85	1.62
Si	0.63	0.28
P	0.045	0.044
S	0.015	0.010
Ti	------	0.019
Nb	------	0.032
Cu	------	0.560
Co	------	0.218
B	------	0.0017
W	------	< 0.055
Sn	------	< 0.004
Pb	------	< 0.006
As	------	< 0.006
Al	------	0.030
V	------	0.064

Table 2: The values of the shape parameter m and the scale parameter n obtained using PSD values as well as using regression analysis (10d exposure)

Specimen	Using PSD values		Using Standard Deviation	
	m (–)	n (s^m)	m (–)	n (s^m)
316SS	**7.50×10^{-2}**	**0.556**	**0.408**	**0.156**
316L(N)	**9.43×10^{-2}**	**0.545**	**0.177**	**0.258**

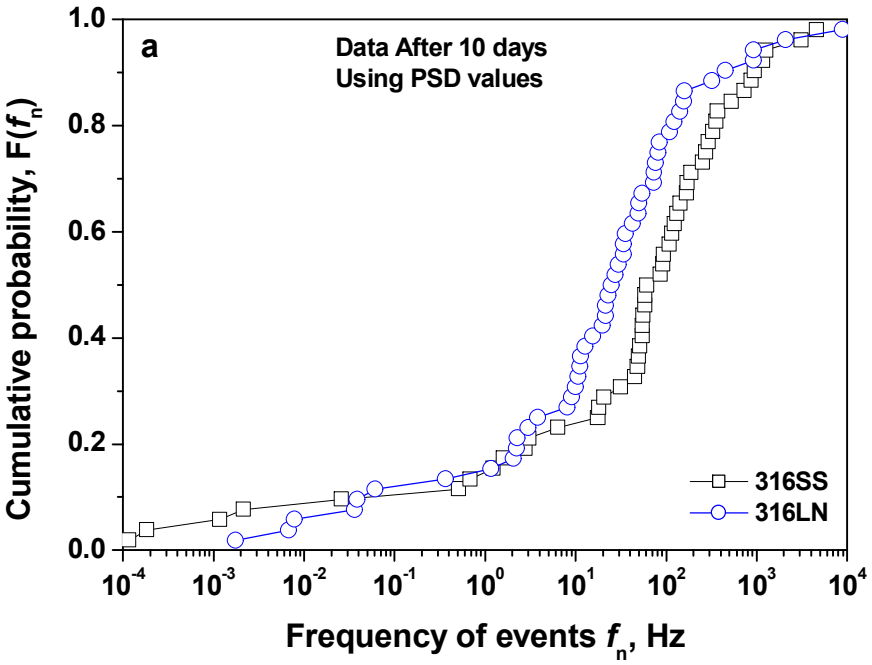
a
Data After 10 days
Using PSD values
316SS
316LN
Cumulative probability, F(f_n)
Frequency of events f_n, Hz
1.0
0.8
0.6
0.4
0.2
0.0
10^-4
10^-3
10^-2
10^-1
10^0
10^1
10^2
10^3
10^4

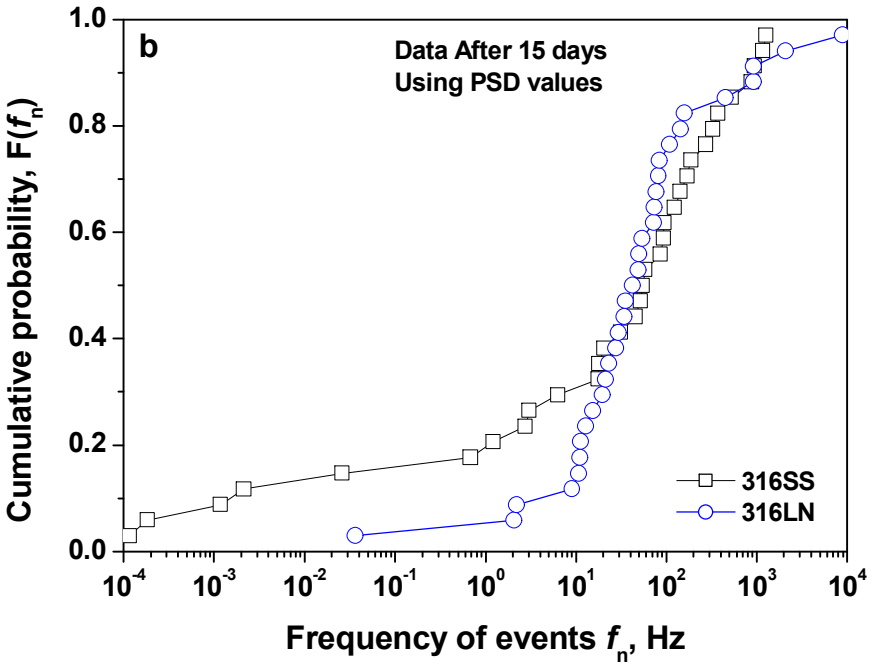
b
Data After 15 days
Using PSD values
316SS
316LN
Cumulative probability, F(f_n)
Frequency of events f_n, Hz
1.0
0.8
0.6
0.4
0.2
0.0
10^-4
10^-3
10^-2
10^-1
10^0
10^1
10^2
10^3
10^4

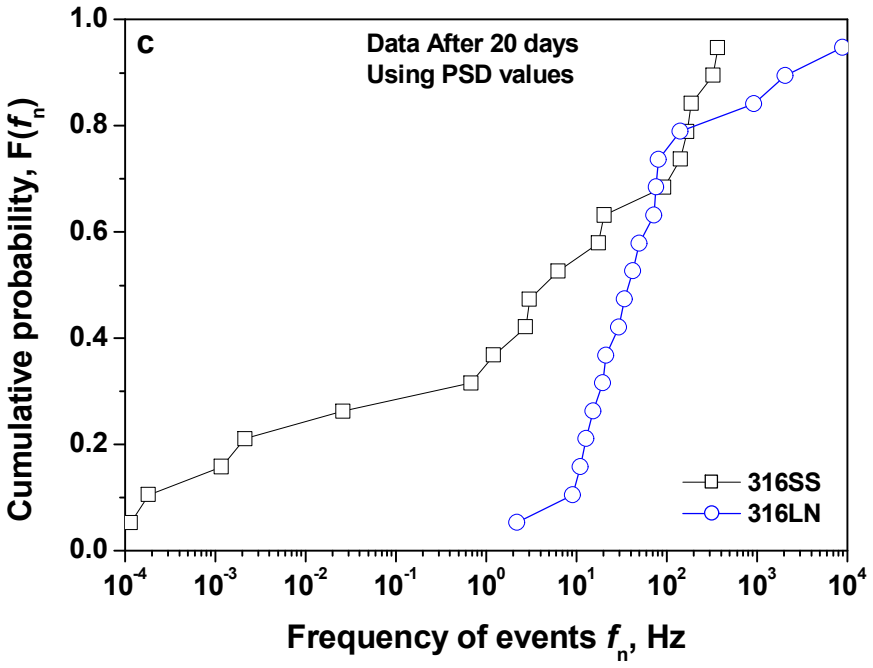

Fig.1 Plots of cumulative probability, F(f_n) versus the frequency of events, f_n for 316SS and 316L(N) in aerated 0.5M NaCl solution, after (a) 10d, (b) 15d and (c) 20d.

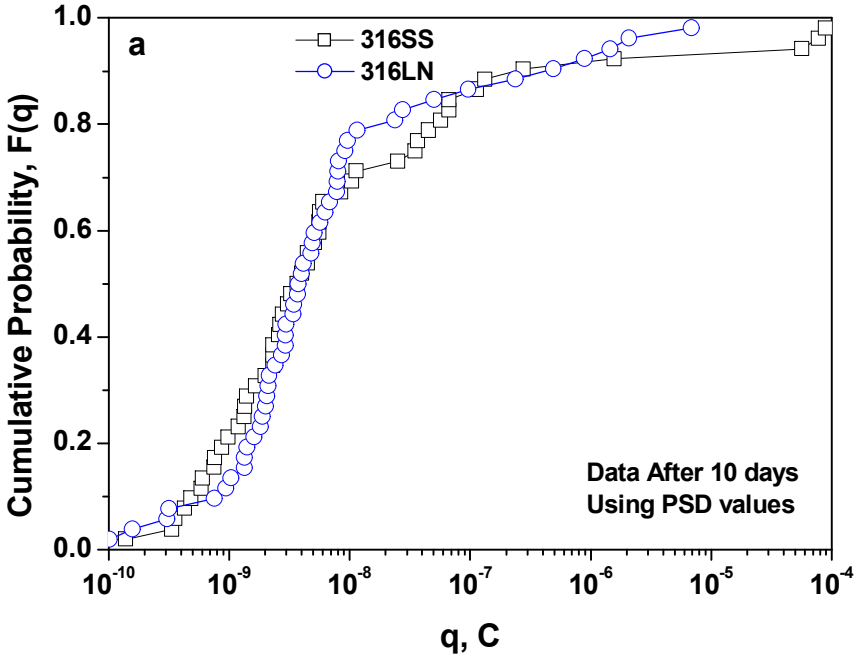

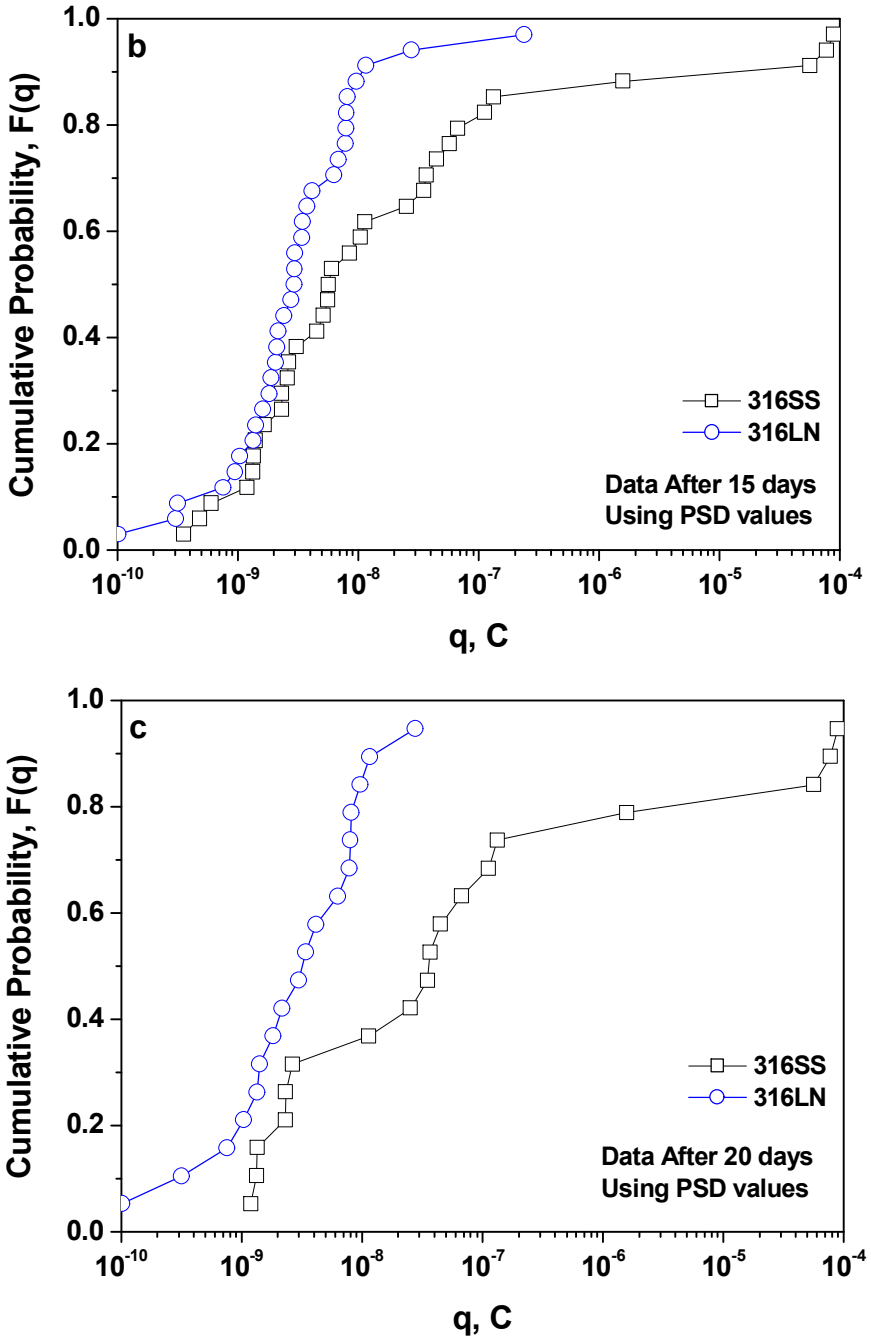

Fig.2 Plots of cumulative probability, F(q) versus the charge, q for 316SS and 316L(N) in aerated 0.5M NaCl solution, after (a) 10d, (b) 15d and (c) 20d.

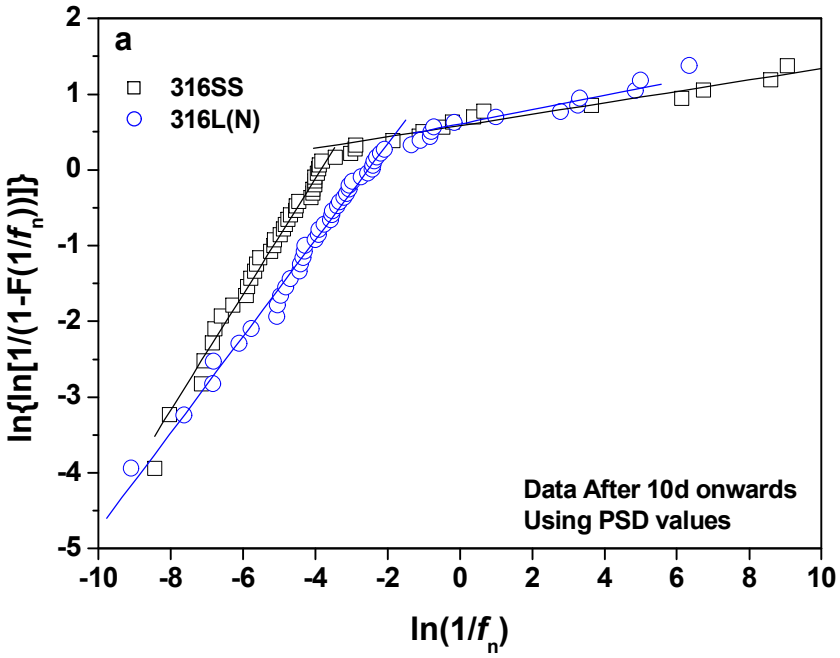
a
316SS
316L(N)
Data After 10d onwards
Using PSD values
ln{ln[1/(1-F(1/f_n))]}
ln(1/f_n)

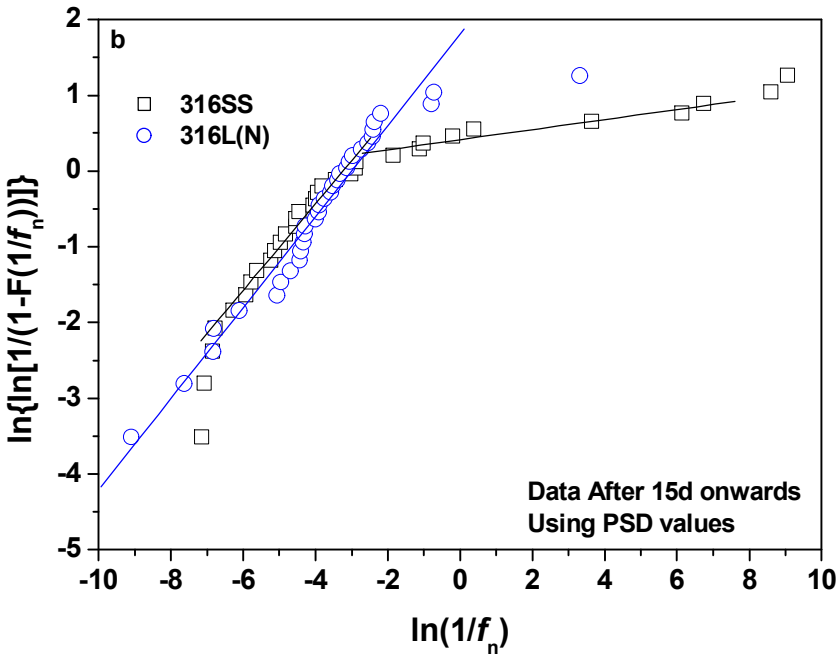
b
316SS
316L(N)
Data After 15d onwards
Using PSD values
ln{ln[1/(1-F(1/f_n))]}
ln(1/f_n)

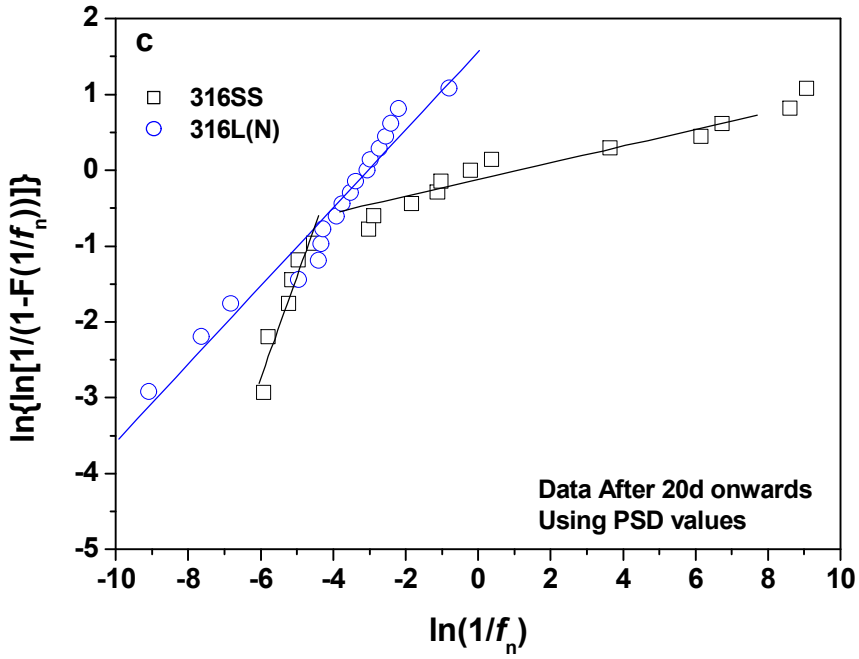

Fig.3 **Weibull Plots (plots of (ln{ln[1/(1-F(1/f_n))]}) vs. ln(1/f_n)) for 316SS and 316L(N) in aerated 0.5M NaCl solution, after (a) 10d, (b) 15d and (c) 20d.**

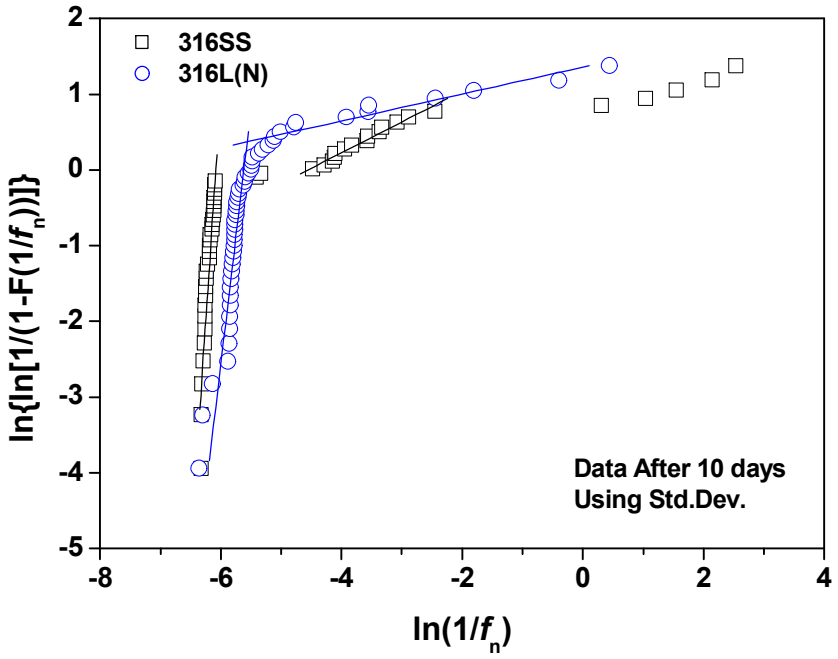

Fig.4 **Weibull Plot (plot of (ln{ln[1/(1-F(1/f_n))]}) vs. ln(1/f_n)) for 316SS and 316L(N) in aerated 0.5M NaCl solution after 10d exposure using standard deviation values**

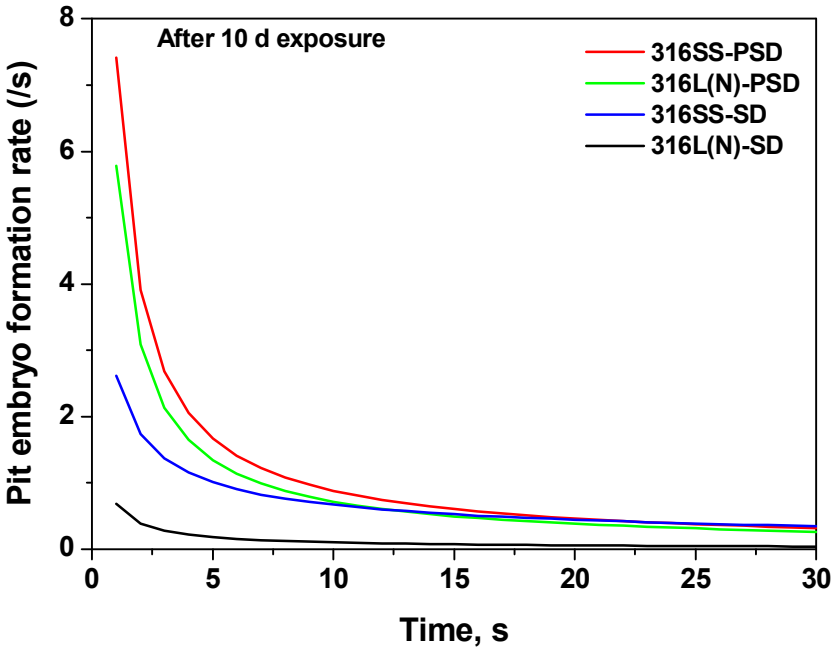

Fig.5 **The plot of pit embryo generation rate, r(t) versus time t for 316SS and 316L(N) in aerated 0.5M NaCl solution after 10d exposure from Weibull Plots using PSD values (WP) as well as standard deviation (SD) values.**

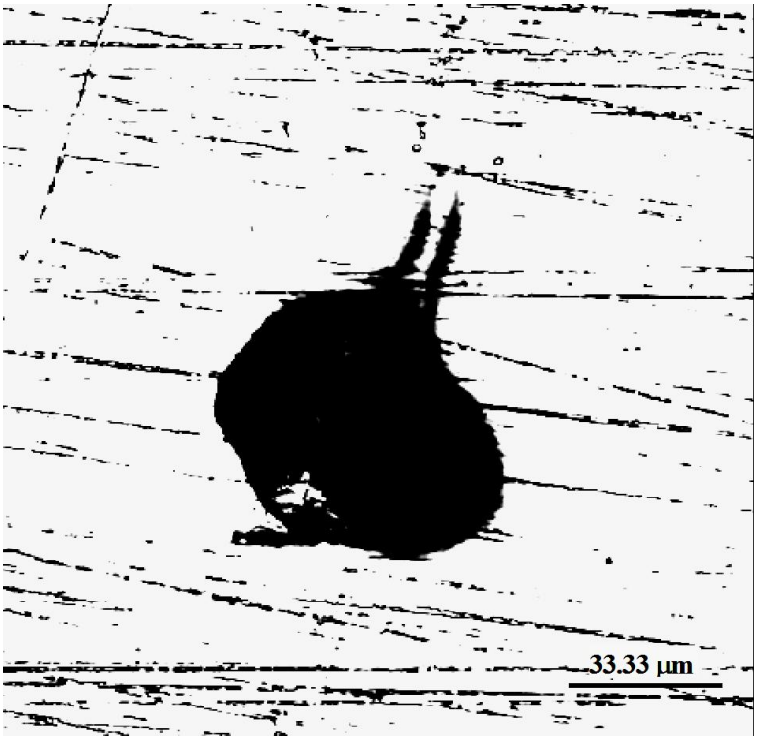

(a)

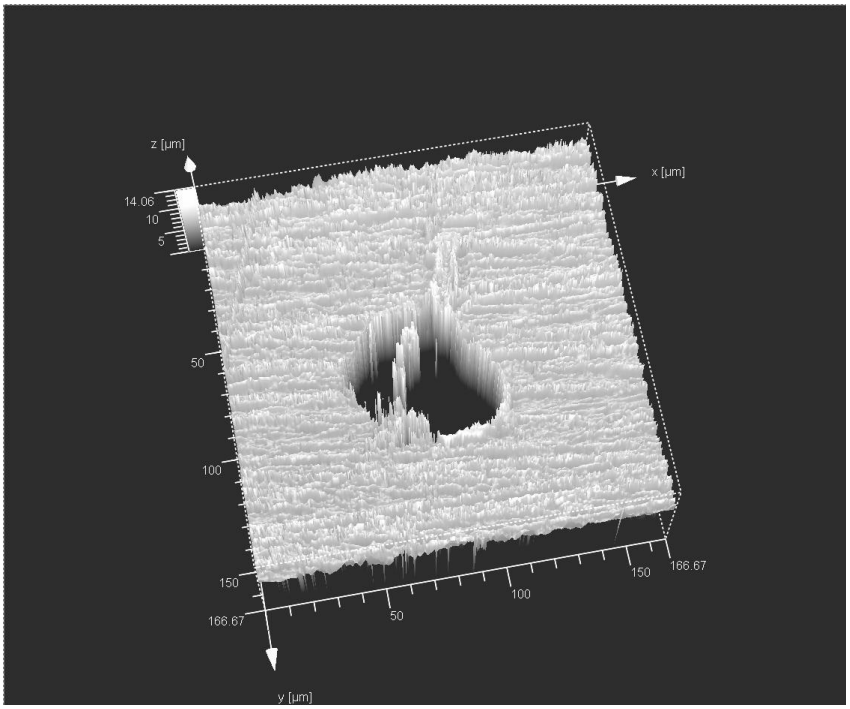

(b)

Fig.6 CLSM photomicrographs for 316SS after 30d exposure showing (a) 2D view of a large pit (b) 3D view of the same pit

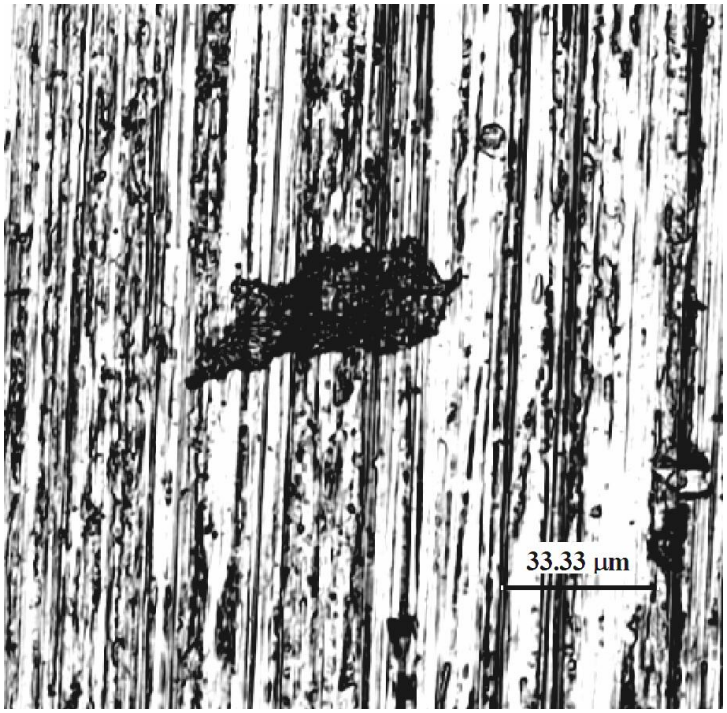

(a)

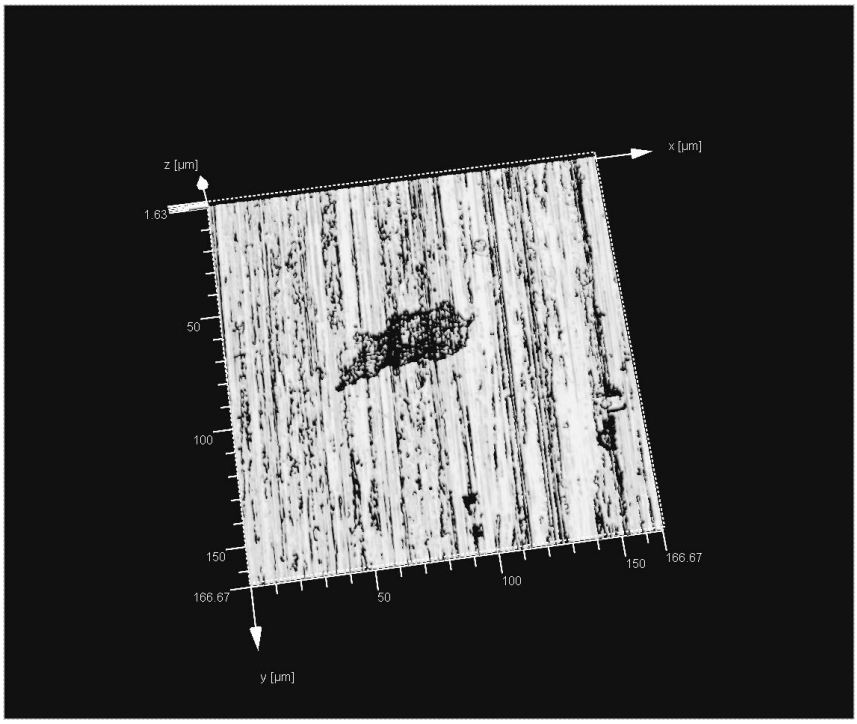

(b)

Fig.7 CLSM photomicrographs for 316L(N) after 30d exposure showing (a) 2D view of a large pit (b) 3D view of the same pit